Applied Mathematics and Computation xxx (2010) xxx–xxx

Contents lists available at ScienceDirect

Applied Mathematics and Computation

journal homepage: www.elsevier.com/locate/amc

Klein–Gordon equation with advection on unbounded domains using spectral elements and high-order non-reflecting boundary conditions

Joseph M. Lindquist *, Francis X. Giraldo, Beny Neta

Department of Applied Mathematics, Naval Postgraduate School, 833 Dyer Road, Monterey, CA 93943, United States

ARTICLE INFO

Keywords:
Klein–Gordon equation
Advection
High-order
Non-reflecting boundary condition
Spectral elements
Higdon
Givoli–Neta
Runge–Kutta

ABSTRACT

A reduced shallow water model under constant, non-zero advection in the infinite channel is considered. High-order (Givoli–Neta) non-reflecting boundary conditions are introduced in various configurations to create a finite computational space and solved using a spectral element formulation with high-order time integration. Numerical examples are used to demonstrate the synergy of using high-order spatial, time, and boundary discretization. We show that by balancing all numerical errors involved, high-order accuracy can be achieved for unbounded domain problems.

Published by Elsevier Inc.

1. Introduction

The numerical solution of a wave propagation problem in a very large or unbounded domain provides a challenging computational difficulty – namely, solving the problem on a finite computational domain while maintaining the true *essence* of the solution. One of the modern techniques that has garnered a significant amount of attention in handling this challenge is the absorbing or non-reflecting boundary condition (NRBC) method. In using this method, the original infinite domain is truncated by an artificial boundary $\mathcal{B}$, resulting in a finite computational domain Ω and the residual domain D.

When truncating the domain, the modeler must devise boundary conditions for the truncated domain. Of course, by imposing a boundary where one does not physically exist, the problem is changed – and unless chosen carefully, would certainly be expected to pollute the solution as the problem evolves and impinges on the boundary. Therefore, two main possibilities exist for the modeler:

- Choose a convenient, easily implementable boundary condition that does not necessarily reflect the physical problem and solve it on a large sub-domain. The idea behind this technique is that the boundary effects are negligible for a short time evolution of the problem in a small area of interest away from the boundaries.
- Choose a boundary condition that preserves the true *behavior* of the infinite solution at the boundary and solve the problem on a smaller sub-domain. The idea behind this technique is that the additional effort extended to impose a better boundary condition will be worth the effort and allow for solving the problem on a smaller domain.

For obvious reasons, the first possibility has only limited usefulness. To see why, suppose that we wanted to model the wave motion following a pebble dropped in the center of a large, still pond. Now, suppose that we have a truncated domain to model this phenomena – say a bathtub. If the pebble is dropped in the bathtub, the waves generated by the pebble would propagate much like that in the pond – until, that is – the wave front reaches the hard walls of the bathtub. At this point, the

* Corresponding author.
E-mail addresses: jmlindqu@nps.edu, joseph.lindquist@us.army.mil (J.M. Lindquist).

0096-3003/$ - see front matter Published by Elsevier Inc.
doi:10.1016/j.amc.2010.07.079

bathtub model ceases to be a useful representation of the pond due to behavior caused by the non-physical boundary. If the modeler wishes to see what happens a short time later – a larger bathtub would be required. This same principle would apply for the numerical solution of this propagation problem – a poor choice of boundary condition mandates the use of a larger computational domain. This in turn, requires additional computational resources. For this reason, much effort has and continues to be exerted on finding stable, efficient, accurate and practical means of reducing this reflection through so-called NRBCs [1].

Several *high-order* NRBCs have been devised to reduce spurious reflections that would pollute the solution. Beginning in the late 1980's, the well-known Engquist–Majda [2] and Bayliss–Turkel conditions [3] gave way to Collino's [4] low derivative, auxiliary variable formulation for the 2D scalar wave equation. This sparked a flurry of activity in an effort to find quality, high-order NRBCs that were easily implementable. See [5–8] for reviews on the subject.

The starting point for the family of NRBCs discussed here is the condition devised by Higdon in a series of papers [9–14], which was demonstrated in a low-order finite difference setting. While in theory, Higdon's NRBC is considered a high-order NRBC, the formulation requires evaluation of increasing high-order spatial and temporal derivatives as the order of the NRBC increased. In [15] Givoli and Neta directly extended the Higdon scheme to high-order finite difference discretizations via an algorithm where the order of the NRBC was simply an input parameter. Long term stability using this formulation was demonstrated in [16]. They later extended this formulation to one that does not involve any high derivatives (hereafter referred to as the G–N formulation). The elimination of all high-order derivatives is enabled through the introduction of special auxiliary variables on $\mathcal{B}$. This construction demonstrated in [17,18] for finite differences was further extended in [19] for finite element schemes to solve the dispersive wave equation.

Hagstrom and Warburton [20] (H–W) also used the Higdon and auxiliary variable framework to develop a symmetric boundary formulation in a full-space configuration where special corner compatibility conditions were developed for the non-dispersive wave equation. One reviewer pointed out a recently published article by Bécache et al. [21] where the H–W formulation is extended for anisotropic and convective wave equations in a finite element setting. Results are presented for the anisotropic case demonstrating significant improvements as the order of the NRBC is increased, although convergence appears to be limited by the numerical discretization.

Several extensive comparisons of the G–N and H–W formulations [21–23] have shown certain advantages of the H–W formulation. One such advantage of the H–W formulation is that the auxiliary variables are shown to decay as the order of the NRBC is increased. While this property is not required for convergence, it is a useful property if dynamic adjustment of the NRBC order is desired. Additionally, while both the G–N and H–W formulations decay exponentially fast as a function of the NRBC order, the H–W formulation has a reflection coefficient that decays twice as fast as the G–N formulation [22, p. 3676]. On the other hand, the G–N formulation is convenient in that through a judicious choice of NRBC parameters, the G–N formulation can be reduced to a first-order (in time) system which is extremely sparse in nature and quite easy to implement. This choice of NRBC parameters does not hamper convergence properties of the boundary scheme.

To see how these auxiliary variable formulations are constructed, consider Fig. 1 that illustrates the NRBC set-up using an infinite wave-guide. Here, the artificial boundary $\mathcal{B}$ extends from the southern (Γ_S) to the northern (Γ_N) boundaries of the wave-guide, thus creating the east (Γ_E) and west (Γ_W) boundaries of Ω at $x = x_E, x_W$ respectively. Outside of the area enclosed by these boundaries is the residual infinite domain D.

Once a suitable NRBC is devised, the problem is solved numerically in Ω, by the finite difference, or, as in the case of this analysis, the spectral element (SE) method. The SE method, originally introduced by Patera, "... combines the generality of the finite element method with the accuracy of spectral techniques..." [24, p. 468]. This generalized high-order finite element method selects the integration and interpolation points carefully in order to yield accurate but efficient solutions. See e.g. Giraldo–Restelli [25] for more details on this method.

In the present paper, the G–N auxiliary formulation of the Higdon NRBC is implemented on a reduced form of the linearized shallow water equations (SWE) under non-zero advection. This formulation has been previously demonstrated in a finite difference formulation to *arbitrarily high* NRBC order [26], however, accuracy gains realized by increasing the NRBC ceased after order 2. The formulation used here seeks to remedy this limitation by using a high-order treatment of space (SE) and time (Runge–Kutta) to show the benefits of using the high-order boundary (G–N) scheme. Specifically, the interior

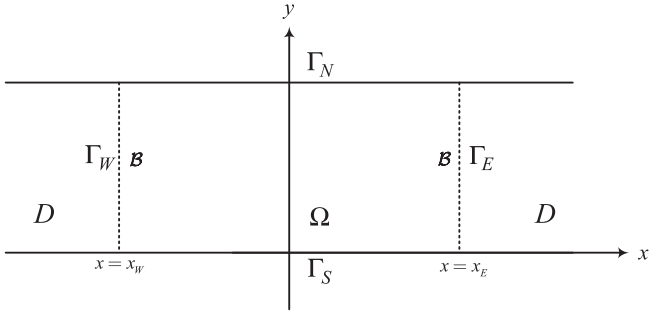

Fig. 1. An infinite wave-guide truncated by artificial boundaries Γ_W and Γ_E.

Please cite this article in press as: J.M. Lindquist et al., Klein–Gordon equation with advection on unbounded domains using spectral elements and high-order non-reflecting boundary conditions, Appl. Math. Comput. (2010), doi:10.1016/j.amc.2010.07.079

and boundary formulations are discretized using high-order basis functions in a stable, equal-order interpolation scheme for all the variables (this does not violate the inf-sup condition). High-order time integration is performed as well in an effort to balance all of the errors involved with the numerical solution. The computational effort associated with the high-order boundary scheme can be shown to grow only *linearly* with the order [19].

It should be noted that the only other spectral element, high-order boundary approach (to the authors' knowledge) are Kucherov and Givoli [27] and Lindquist et al. [28]. Kucherov and Givoli demonstrate exponential error convergence of the classical wave equation on a semi-infinite channel when solved using spectral elements and high-order boundary treatment (using the H–W boundary scheme). They further show how the spectral element formulation allows the NRBC to realize its true potential, prior masked by low-order numerical schemes. They note that, "Although it is generally felt that there is no need to treat the time domain 'spectrally' like the spatial domain, [they] feel that a consistently high-order treatment requires that the *entire* approximation be spectral, i.e. the convergence of all three types of error – the spatial and temporal discretization errors and the ABC error – be exponential." [27]

Subsequent spectral element and boundary work by the current authors [28] using the G–N formulation of the dispersive wave equation on a semi-infinite channel showed similar results to those presented by Kucherov and Givoli and how a high-order treatment of the time domain (up to order 10) produces additional improvements. These improvements, however, have their limits thus confirming the hypothesis of Kucherov and Givoli. The key difference in this work is that we extend the high-order space, boundary *and* time integration results previously demonstrated in a non-zero advection setting to one where the wave medium is not at rest.

The following is the outline of the rest of this paper. In Section 2, the problem under investigation is stated. In Section 3, an overview of the G–N auxiliary formulation is presented. In Section 4, a SE semi-discrete formulation that incorporates the G–N NRBC with any desired order is constructed. In Section 5 the time-integrator used to March the equations in time is discussed. The performance of the method is demonstrated in Section 6 via numerical examples.

2. Statement of the problem

To motivate the problem under consideration, consider the SWE:

$$\begin{aligned} &\partial_t u + u\partial_x u + v\partial_y u - f v = -g\partial_x \eta, \\ &\partial_t v + u\partial_x v + v\partial_y v + fu = -g\partial_y \eta, \\ &\partial_t \eta + \partial_x (Hu) + \partial_y (Hv) = 0. \end{aligned} \tag{1}$$

We use the following shorthand for partial derivatives

$$\partial_a^i = \frac{\partial^i}{\partial a^i}.$$

The shallow water model in its current form is non-linear. We have three state variables: $u(x,y,t)$ and $v(x,y,t)$ are the unknown velocities in the x and y directions and $\eta(x,y,t)$ is the water depth above a reference value. Further, H is the water depth as shown in Fig. 2 such that $H = h_B + \eta$, f is the Coriolis parameter, and g is the gravity acceleration. Now, suppose that the bottom topography is flat such that h_B is constant and u and v can be described by a constant *mean* term and a small $O(\delta)$ deviation from that value, i.e.

$$u = U + u^* \quad v = V + v^*.$$

To be clear, U and V are the mean velocities with respect to the coordinate axes. Using these substitutions and neglecting any $O(\delta^2)$ terms results in the linearized form of the SWE:

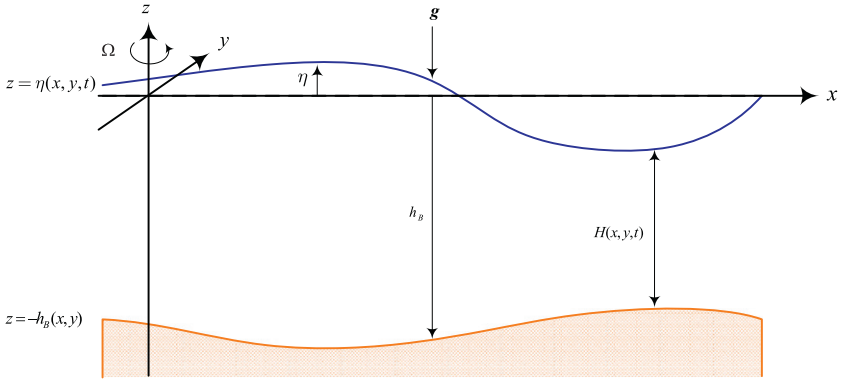

Fig. 2. The shallow water model with irregular bottom topography. (Adapted from [29, p. 58]).

Please cite this article in press as: J.M. Lindquist et al., Klein–Gordon equation with advection on unbounded domains using spectral elements and high-order non-reflecting boundary conditions, Appl. Math. Comput. (2010), doi:10.1016/j.amc.2010.07.079

$$\begin{aligned}
&\partial_t u^* + U\partial_x u^* + V\partial_y u^* - f(V + v^*) = -g\partial_x \eta,\\
&\partial_t v^* + U\partial_x v^* + V\partial_y v^* + f(U + u^*) = -g\partial_y \eta,\\
&\partial_t \eta + U\partial_x \eta + V\partial_y \eta + h_B(\partial_x u^* + \partial_y v^*) = 0.
\end{aligned} \tag{2}$$

van Joolen shows in [30], how, using the operator:

$$\frac{D}{Dt} = \frac{\partial}{\partial t} + U\frac{\partial}{\partial x} + V\frac{\partial}{\partial y},$$

the SWE can be reduced to a single variable Klein Gordon equation (KGE) equivalent for the wave perturbation η under non-zero, constant advection velocities U and V. Once η has been found, the unknown velocities can be computed in a similar manner (see [29] for details). This work seeks to numerically solve this two-dimensional advective, dispersive wave equation:

$$\partial_t^2\eta + \left(U^2 - C_0^2\right)\partial_x^2\eta + \left(V^2 - C_0^2\right)\partial_y^2\eta + 2U\partial_{xt}^2\eta + 2V\partial_{yt}^2\eta + 2UV\partial_{xy}^2\eta + f^2\eta = 0, \tag{3}$$

where $C_0^2 = gH$, using continuous Galerkin methods.

While the assumptions for this reduced form of the SWE may undermine the predictive capability of the already simplified equations of fluid motion, the advective KGE serves as an important test-bed to extend and improve non-reflecting boundary conditions for wave propagation in a non-static environment. When shown to improve performance in test cases as those presented here, these conditions will then be extended to the full linearized SWE system and further to include non-linear effects.

We begin this analysis by considering the semi-infinite wave-guide where Dirichlet boundary conditions $\eta(0,y,t) = f(y,t)$ are prescribed on Γ_W, no-flux boundary conditions $\frac{\partial \eta}{\partial y} = 0$ on Γ_N and Γ_S and the G–N NRBCs are enforced on Γ_E. Further, initial data $\eta(x,y,0)$ and $\partial_t\eta(x,y,0)$ are prescribed at $t = 0$. The set-up is illustrated in Fig. 3.

3. G–N auxiliary variable formulation

We present a brief summary of the G–N auxiliary variable process as described in [19]. This auxiliary formulation begins with the Higdon [14] boundary condition given by:

$$H_J : \left[\prod_{j=1}^{J}\left(\partial_x + \frac{1}{C_j}\partial_t\right)\right]\eta = 0 \quad \text{on } \Gamma_E. \tag{4}$$

Note that the first-order condition $J = 1$ corresponds to the Sommerfeld radiation condition, provided that $C_j = C_0$. Auxiliary functions $\phi_1, \ldots, \phi_{J-1}$, which are defined on Γ_E as well as in the exterior domain D (see Fig. 3) are now introduced. Eventually we shall use these functions only on Γ_E, but the derivation requires that they be defined in D as well, or at least in a non-vanishing region adjacent to Γ_E. The functions ϕ_j are defined via the relations

$$\left(\partial_x + \frac{1}{C_1}\partial_t\right)\eta = \phi_1, \tag{5}$$

$$\left(\partial_x + \frac{1}{C_2}\partial_t\right)\phi_1 = \phi_2, \tag{6}$$

$$\vdots$$

$$\left(\partial_x + \frac{1}{C_J}\partial_t\right)\phi_{J-1} = 0. \tag{7}$$

By definition, these relations hold in D, and also on Γ_E. It is easy to see that (5)–(7), when imposed as boundary conditions on Γ_E, are equivalent to the single boundary condition (4). If we also define

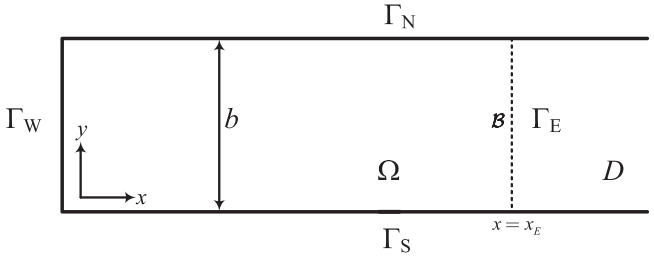

Fig. 3. A semi-infinite channel domain Ω truncated by artificial boundary Γ_E.

Please cite this article in press as: J.M. Lindquist et al., Klein–Gordon equation with advection on unbounded domains using spectral elements and high-order non-reflecting boundary conditions, Appl. Math. Comput. (2010), doi:10.1016/j.amc.2010.07.079

$$\phi_0 \equiv \eta \quad \phi_J \equiv 0, \tag{8}$$

then we can write (5)–(7) concisely as:

$$\left(\partial_x + \frac{1}{C_j}\partial_t\right)\phi_{j-1} = \phi_j \quad j = 1,\ldots,J. \tag{9}$$

This set of conditions involves only first-order derivatives. However, due to the appearance of the x-derivative in (9), one cannot discretize the ϕ_j on the boundary Γ_E alone. Therefore, we shall manipulate (9) in order to get rid of the x-derivative.

The function η satisfies the dispersive, advective wave Eq. (3) in D. Since the function ϕ_1 is obtained by applying the linear (constant coefficient) operator $\left(\partial_x + \frac{1}{C_1}\partial_t\right)$ to η, it is clear that ϕ_1 should also satisfy the same equation in D. Further, since ϕ_j is obtained by applying the same linear operator $j-1$ times to ϕ_1, the functions ϕ_j should satisfy an equation like Eq. (3), namely,

$$\partial_t^2\phi_j + \left(U^2 - C_0^2\right)\partial_x^2\phi_j + \left(V^2 - C_0^2\right)\partial_y^2\phi_j + 2U\partial_{xt}^2\phi_j + 2V\partial_{yt}^2\phi_j + 2UV\partial_{xy}^2\phi_j + f^2\phi_j = 0. \tag{10}$$

Using the following identities:

$$\partial_x^2\phi_j = \left(\partial_x - \frac{1}{C_{j+1}}\partial_t\right)\left(\partial_x + \frac{1}{C_{j+1}}\partial_t\right)\phi_j + \frac{1}{C_{j+1}^2}\ddot{\phi}_j,$$
$$\partial_{xt}^2\phi_j = \partial_t(\partial_x\phi_j),$$
$$\partial_{xy}^2\phi_j = \partial_y(\partial_x\phi_j)$$

and combining with (10) allows us to write (9) as:

$$\left(\frac{2U}{C_j} - 1 - \frac{U^2 - C_0^2}{C_j^2}\right)\ddot{\phi}_{j-1} + \left(\frac{2UV}{C_j} - 2V\right)\dot{\phi}'_{j-1} - \left(V^2 - C_0^2\right)\phi''_{j-1}$$
$$+ \left(\left(U^2 - C_0^2\right)\left(\frac{1}{C_j} + \frac{1}{C_{j+1}}\right) - 2U\right)\dot{\phi}_j - 2UV\phi'_j - f^2\phi_{j-1} = \left(U^2 - C_0^2\right)\phi_{j+1} \quad \text{for } j = 1,\ldots,J-1. \tag{11}$$

In (11) and elsewhere, a prime indicates differentiation with respect to y along Γ, i.e. the tangential derivative along Γ. As desired, the new boundary condition (11) does not involve x-derivatives. In addition, there are no high-y or t derivatives beyond second order. It should be noted that van Joolen et al. [26] developed an equivalent formulation using Lagrangian derivatives.

Rewriting (5), (11) and (8), the new formulation of the Jth-order NRBC on Γ can be summarized as follows:

$$\beta_0\dot{\eta} + \partial_x\eta = \phi_1, \tag{12}$$
$$\alpha_j\ddot{\phi}_{j-1} + \zeta_j\dot{\phi}'_{j-1} - \lambda_y\phi''_{j-1} + \beta_j\dot{\phi}_j - \gamma\phi'_j - f^2\phi_{j-1} = \lambda_x\phi_{j+1}, \tag{13}$$
$$\phi_0 \equiv \eta \quad \phi_J \equiv 0, \tag{14}$$
$$\beta_0 = \frac{1}{C_1}, \quad \alpha_j = \frac{2U}{C_j} - 1 - \frac{U^2 - C_0^2}{C_j^2}, \quad \zeta_j = \frac{2UV}{C_j} - 2V, \quad \lambda_y = V^2 - C_0^2,$$
$$\beta_j = \left(U^2 - C_0^2\right)\left(\frac{1}{C_j} + \frac{1}{C_{j+1}}\right) - 2U, \quad \gamma = 2UV, \quad \lambda_x = U^2 - C_0^2.$$

4. Spectral element method

The spectral element (SE) method is a generalized high-order finite element method where the integration and interpolation points are selected carefully in order to yield accurate but efficient solutions. For this problem, we will discuss two formulations-one for the interior and one for implementing the boundary conditions.

4.1. Interior formulation

The weak form of the problem in Ω is constructed. The solution is sought in the space of trial functions,

$$\mathcal{V} = \{\eta | \eta \in H^1(\Omega) \text{ and } \eta = 0 \text{ on } \Gamma_W\}. \tag{15}$$

Here, $H^1(\Omega)$ is the Sobolev space of functions whose first derivatives are also square-integrable in Ω. Now, Eq. (3) is multiplied by the basis functions $\Psi_i(x,y) \in \mathcal{V}$ and integrated over Ω so the weak form is:

Please cite this article in press as: J.M. Lindquist et al., Klein–Gordon equation with advection on unbounded domains using spectral elements and high-order non-reflecting boundary conditions, Appl. Math. Comput. (2010), doi:10.1016/j.amc.2010.07.079

$$\int_\Omega \Psi_i \ddot{\eta}\, d\Omega + \lambda_x \int_\Omega \Psi_i \partial_x^2 \eta\, d\Omega + \lambda_y \int_\Omega \Psi_i \partial_y^2 \eta\, d\Omega + 2U \int_\Omega \Psi_i \partial_x \dot{\eta}\, d\Omega + 2V \int_\Omega \Psi_i \partial_y \dot{\eta}\, d\Omega + UV \int_\Omega \Psi_i \partial_{xy}^2 \eta\, d\Omega + UV \int_\Omega \Psi_i \partial_{yx}^2 \eta\, d\Omega + f^2 \int_\Omega \Psi_i \eta\, d\Omega = 0. \tag{16}$$

In order to maintain a symmetric form of the problem, the mixed derivative has been split appropriately. To ensure the solution η is in the vector space H^1 requires some special handling of the second order derivatives, which is facilitated by the use of Green's theorem, i.e.

$$\int_\Omega \Psi_i \partial_x^2 \eta\, d\Omega = \int_\Gamma \Psi_i \partial_x \eta n_x d\Gamma - \int_\Omega \partial_x \Psi_i \partial_x \eta\, d\Omega, \tag{17}$$

where $\vec{n}$ is the outward normal on Γ and n_x is the x-component of that outward normal.

Extending this idea for each second order derivative in (16) gives the weak form:

$$\int_\Omega \Psi_i \ddot{\eta}\, d\Omega - \lambda_x \int_\Omega \partial_x \Psi_i \partial_x \eta\, d\Omega - \lambda_y \int_\Omega \partial_y \Psi_i \partial_y \eta\, d\Omega - UV \int_\Omega \partial_y \Psi_i \partial_x \eta\, d\Omega - UV \int_\Omega \partial_x \Psi_i \partial_y \eta\, d\Omega + 2U \int_\Omega \Psi_i \partial_x \dot{\eta}\, d\Omega + 2V \int_\Omega \Psi_i \partial_y \dot{\eta}\, d\Omega + f^2 \int_\Omega \Psi_i \eta\, d\Omega + \lambda_x \int_\Gamma \Psi_i \partial_x \eta n_x\, d\Gamma + \lambda_y \int_\Gamma \Psi_i \partial_y \eta n_y\, d\Gamma + UV \int_\Gamma \Psi_i \partial_x \eta n_y\, d\Gamma + UV \int_\Gamma \Psi_i \partial_y \eta n_x\, d\Gamma = 0. \tag{18}$$

Using the no-flux boundary conditions on the northern and southern borders along with the normal vectors specified by the structured, rectangular grid shown in Fig. 4, the problem may be simplified to account for contributions on individual boundaries. Using this information along with (12) to eliminate the normal derivative term on Γ_E, we get:

$$\int_\Omega \Psi_i \ddot{\eta}\, d\Omega - \lambda_x \int_\Omega \partial_x \Psi_i \partial_x \eta\, d\Omega - \lambda_y \int_\Omega \partial_y \Psi_i \partial_y \eta\, d\Omega - UV \int_\Omega \partial_y \Psi_i \partial_x \eta\, d\Omega - UV \int_\Omega \partial_x \Psi_i \partial_y \eta\, d\Omega + 2U \int_\Omega \Psi_i \partial_x \dot{\eta}\, d\Omega + 2V \int_\Omega \Psi_i \partial_y \dot{\eta}\, d\Omega + f^2 \int_\Omega \Psi_i \eta\, d\Omega + \lambda_x \int_{\Gamma_E} \Psi_i \phi_1\, d\Gamma_E - \beta_0 \lambda_x \int_{\Gamma_E} \Psi_i \dot{\eta}\, d\Gamma_E + UV \int_{\Gamma_N} \Psi_i \partial_x \eta\, d\Gamma_N - UV \int_{\Gamma_S} \Psi_i \partial_x \eta\, d\Gamma_S + UV \int_{\Gamma_E} \Psi_i \partial_y \eta\, d\Gamma_E = 0. \tag{19}$$

4.2. Boundary formulation

Since the term ϕ_1 appears in the interior formulation (19), this is not a complete weak form of the problem in Ω. We turn our attention to computing a separate weak form for (13) to complete the problem statement.

As in the interior formulation, we multiply (13) by the test function τ_j and integrate it over Γ_E. After integration by parts and simplifying yields:

$$\alpha_j \int_{\Gamma_E} \tau_i \ddot{\phi}_{j-1}\, d\Gamma_E + \zeta_j \int_{\Gamma_E} \tau_i \dot{\phi}'_{j-1}\, d\Gamma_E + \lambda_y \int_{\Gamma_E} \tau_i \phi_{j-1}'\, d\Gamma_E + \beta_j \int_{\Gamma_E} \tau_i \dot{\phi}_j\, d\Gamma_E - \gamma \int_{\Gamma_E} \tau_i \phi'_j\, d\Gamma_E - f^2 \int_{\Gamma_E} \tau_i \phi_{j-1}\, d\Gamma_E = \lambda_x \int_{\Gamma_E} \tau_i \phi_{j+1}\, d\Gamma_E \tag{20}$$

for $j = 1, \ldots, J-1$, $\phi_j \in H^1(\Gamma_E)$ and any $\tau_i \in H^1(\Gamma_E)$. Recall from the auxiliary variable formulation (14) that $\phi_0 \equiv \eta$ and $\phi_J \equiv 0$.

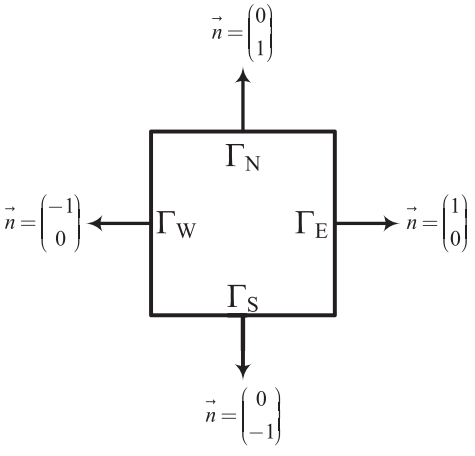

Fig. 4. Normal derivatives to boundaries.

Please cite this article in press as: J.M. Lindquist et al., Klein–Gordon equation with advection on unbounded domains using spectral elements and high-order non-reflecting boundary conditions, Appl. Math. Comput. (2010), doi:10.1016/j.amc.2010.07.079

The formal problem statement is then: Find $\eta \in \mathcal{V}$ and $\phi_j \in H^1(\Gamma_E)$, $j = 1,\ldots,J-1$, such that Eqs. (19) and (20) are satisfied $\forall \Psi_i \in \mathcal{V}$ and $\tau_i \in H^1(\Gamma_E)$.

4.3. Galerkin expansion

We now turn our attention to the spatial discretization. First, we expand the solution variables η and ϕ_j using the same basis functions used in the weak form as follows:

$$\eta_N = \sum_{k=1}^{N_p} \Psi_k \eta^k, \quad \phi_{jN} = \sum_{k=1}^{N_b} \tau_k \phi_j^k, \quad j = 1,2,\ldots,J-1. \tag{21}$$

Here, N_p refers to the number of points that Ω is discretized into and N_b refers to the number of points that Γ_E is discretized into. Next, we substitute this basis function expansion directly into the weak form, resulting in the following matrix form of this problem:

$$\begin{aligned} &M\ddot{\eta} + (2UD_x + 2VD_y)\dot{\eta} + \left(-\lambda_x L_{xx} - \lambda_y L_{yy} + f^2 M - UVL_{yx} - UVL_{xy}\right)\eta + \lambda_x A_E \phi_1 - \beta_0 \lambda_x B_E \dot{\eta} \\ &\quad + (UVC_N - UVC_S + UVC_E)\eta = 0, \end{aligned} \tag{22}$$

$$\alpha_j M^b \ddot{\phi}_{j-1} + \zeta_j D^b \dot{\phi}_{j-1} + \left(\lambda_y L^b - f^2 M^b\right)\phi_{j-1} + \beta_j M^b \dot{\phi}_j - \gamma D^b \phi_j = \lambda_x M^b \phi_{j+1} \quad j = 1,\ldots,J-1, \tag{23}$$

where M, D_x, D_y, L_{xx}, L_{yy}, L_{xy} and L_{yx} are interior formulation matrices of size $N_p \times N_p$. Further, B_E, C_N, C_S and C_E are interior formulation matrices integrated along the boundaries of size $N_p \times N_p$ while A_E is of size $N_p \times N_b$. Finally, M^b, D^b and L^b are auxiliary formulation matrices of size $N_b \times N_b$. These global matrices are obtained from analogous element arrays via assembly, given by:

$$\begin{aligned} &M = \bigwedge_{e=1}^{N_e} M^e, \quad B_E = \bigwedge_{e=1}^{N_e} B_E^e, \quad D_x = \bigwedge_{e=1}^{N_e} D_x^e, \quad D_y = \bigwedge_{e=1}^{N_e} D_y^e, \\ &L_{xx} = \bigwedge_{e=1}^{N_e} L_{xx}^e, \quad L_{yy} = \bigwedge_{e=1}^{N_e} L_{yy}^e, \quad L_{xy} = \bigwedge_{e=1}^{N_e} L_{xy}^e, \quad L_{yx} = \bigwedge_{e=1}^{N_e} L_{yx}^e, \\ &M^b = \bigwedge_{b=1}^{N_b} m^b, \quad D^b = \bigwedge_{b=1}^{N_b} d^b, \quad L^b = \bigwedge_{b=1}^{N_b} l^b, \quad C_N = \bigwedge_{e=1}^{N_e} C_N^e, \\ &C_S = \bigwedge_{e=1}^{N_e} C_S^e, \quad C_E = \bigwedge_{e=1}^{N_e} C_E^e, \quad A_E = \bigwedge_{e=1}^{N_e} A_E^e, \end{aligned} \tag{24}$$

where $\bigwedge_{e=1}^{N_e}$ is the direct stiffness summation operator required by all continuous Galerkin methods. The expressions for the element arrays are:

$$\begin{aligned} &M_{ij}^e = \int_{\Omega_e} \psi_i \psi_j \, d\Omega_e \quad B_{E,ij}^e = \int_{\Gamma_e^E} \psi_i \psi_j \, d\Gamma_e^E \quad D_{x,ij}^e = \int_{\Omega_e} \psi_i \partial_x \psi_j \, d\Omega_e, \\ &D_{y,ij}^e = \int_{\Omega_e} \psi_i \partial_y \psi_j \, d\Omega_e \quad L_{xx,ij}^e = \int_{\Omega_e} \partial_x \psi_i \partial_x \psi_j \, d\Omega_e \quad L_{yy,ij}^e = \int_{\Omega_e} \partial_y \psi_i \partial_y \psi_j \, d\Omega_e, \\ &L_{xy,ij}^e = \int_{\Omega_e} \partial_y \psi_i \partial_x \psi_j \, d\Omega_e \quad L_{yx,ij}^e = \int_{\Omega_e} \partial_x \psi_i \partial_y \psi_j \, d\Omega_e \quad m_{rs}^b = \int_{\Gamma_e} v_r v_s \, d\Gamma_e, \\ &d_{rs}^b = \int_{\Gamma_e} v_r v_s' \, d\Gamma_e \quad l_{rs}^b = \int_{\Gamma_e} v_r' v_s' \, d\Gamma_e \quad C_{N,ij}^e = \int_{\Gamma_e^N} \psi_i \partial_x \psi_j \, d\Gamma_e^N, \\ &C_{S,ij}^e = \int_{\Gamma_e^S} \psi_i \partial_x \psi_j \, d\Gamma_e^S \quad C_{E,ij}^e = \int_{\Gamma_e^E} \psi_i \partial_y \psi_j \, d\Gamma_e^E \quad A_{E,ir}^e = \int_{\Gamma_e^E} \psi_i v_r \, d\Gamma_e^E, \end{aligned} \tag{25}$$

where Ω_e and Γ_e denote, the part of Ω and Γ associated with element e. Also, ψ_i and v_i are the locally defined basis functions from which the global basis functions (Ψ_i and τ_i) are formed. For quadrilateral elements with spectral order N as used in this analysis, ψ_i will be discretized into $(N+1)^2$ points, and v_i into $(N+1)$ points, thus, $i, j = 1,2,\ldots,(N+1)^2$ and $r, s = 1,2,\ldots,N+1$.

Now, let:

$$\begin{aligned} &\mathbb{A} = M^{-1}\left[\beta_0 \lambda_x B_E - 2UD_x - 2VD_y\right], \\ &\mathbb{B} = M^{-1}\left[\lambda_x L_x + \lambda_y L_y - f^2 M + UVL_{xy} + UVL_{yx} - UVC_N + UVC_S - UVC_E\right], \\ &\mathbb{C} = -\lambda_x M^{-1} A_E^b \end{aligned} \tag{26}$$

Please cite this article in press as: J.M. Lindquist et al., Klein–Gordon equation with advection on unbounded domains using spectral elements and high-order non-reflecting boundary conditions, Appl. Math. Comput. (2010), doi:10.1016/j.amc.2010.07.079

and substitute Eq. (26) into Eq. (22) to get the matrix form of the interior problem:

$$\ddot{\eta} = \mathbb{A}\dot{\eta} + \mathbb{B}\eta + \mathbb{C}\phi_1. \tag{27}$$

If we examine the boundary auxiliary variable formulation (13) we see that the selection of appropriate C_j values for the auxiliary variables has not yet been addressed. It should be noted that van Joolen et al. [31] show that *any* choice of C_j is guaranteed to reduce spurious reflection as the order of the NRBC (J) increases. While we omit the details here, the core of this argument is the computation of a so-called reflection coefficient that is a product of J factors, each of which are less than one. The reflection caused by the artificial boundary *must* decrease as the order of the NRBC increases. They note, "Of course, a good choice for the C_j would lead to better accuracy with a lower order J, but even if the 'wrong' C_j's are taken... one is still guaranteed to reduce the spurious reflection as the order J increases." [31, p. 1045]

Armed with this, we choose convenient values for our C_j's that cause the second order in time (α_j) terms to vanish. In the case of the semi-infinite channel, on the eastern boundary this value is: $C_j = C_0 + U$. A physical argument for this choice is that since the predominant speed of the wave, absent the advection terms, is C_0, the C_j terms "correct" the boundary formulation to account for the advection. This selection for the C_j's then makes:

$$\begin{aligned}
&\alpha_1 = \alpha_2 = \cdots = \alpha_{J-1} = 0,\\
&\zeta_1 = \zeta_2 = \cdots = \zeta_{J-1} = \zeta,\\
&\beta_1 = \beta_2 = \cdots = \beta_{J-1} = \beta.
\end{aligned}$$

Now, let:

$$\mathbb{D} = f^2 M^b - \lambda_y L^b \tag{28}$$

and substitute (28) into (23) to get the following form of the problem:

$$\begin{aligned}
&\beta M^b \dot{\phi}_1 = \mathbb{D}\eta_\Gamma - \zeta D^b \dot{\eta}_\Gamma + \gamma D^b \phi_1 + \lambda_x M^b \phi_2,\\
&\zeta D^b \dot{\phi}_1 + \beta M^b \dot{\phi}_2 = \mathbb{D}\phi_1 + \gamma D^b \phi_2 + \lambda_x M^b \phi_3,\\
&\zeta D^b \dot{\phi}_2 + \beta M^b \dot{\phi}_3 = \mathbb{D}\phi_2 + \gamma D^b \phi_3 + \lambda_x M^b \phi_4,\\
&\quad\vdots\\
&\zeta D^b \dot{\phi}_{J-2} + \beta M^b \dot{\phi}_{J-1} = \mathbb{D}\phi_{J-2} + \gamma D^b \phi_{J-1}.
\end{aligned} \tag{29}$$

If we now collect the terms on the left and right, we get the matrix form of the problem:

$$\mathbb{E}\dot{\Phi} = \mathbb{F}\Phi + \bar{\eta}, \tag{30}$$

where:

$$\mathbb{E} = \begin{pmatrix} \beta M^b & 0 & \dots & 0\\ \zeta D^b & \beta M^b & \dots & 0\\ \vdots & \vdots & \ddots & \vdots\\ 0 & 0 & \zeta D^b & \beta M^b \end{pmatrix}, \quad \mathbb{F} = \begin{pmatrix} \gamma D^b & \lambda_x M^b & 0 & \dots & 0\\ \mathbb{D} & \gamma D^b & \lambda_x M^b & \dots & 0\\ \vdots & \vdots & \vdots & \ddots & \vdots\\ 0 & 0 & 0 & \mathbb{D} & \gamma D^b \end{pmatrix},$$

$$\Phi = \begin{pmatrix} \phi_1\\ \phi_2\\ \vdots\\ \phi_{J-1} \end{pmatrix}, \quad \dot{\Phi} = \begin{pmatrix} \dot{\phi}_1\\ \dot{\phi}_2\\ \vdots\\ \dot{\phi}_{J-1} \end{pmatrix} \quad \text{and} \quad \bar{\eta} = \begin{pmatrix} \mathbb{D}\eta_\Gamma - \zeta D^b \dot{\eta}_\Gamma\\ 0\\ \vdots\\ 0 \end{pmatrix}.$$

It should be noted that if U and V are taken to be zero, that this entire formulation reduces to the formulation shown by Lindquist et al. [28].

5. Time integration

The formulation outlined in (22) and (23) constitute a system of coupled ODEs that must be solved to yield a solution for $\eta(x,y,t)$. Since the goal of this analysis is to uncover the "true" gains made by high-order boundary treatment, it is possible that any high-order treatment of the boundary and spatial discretization *without* considering a high-order treatment of the temporal component could mask gains made by high-order boundary treatment. For this purpose, our approach uses standard kth order Runge–Kutta (RK) methods (up to order 10) to integrate the system in time.

The set-up of this scheme is a standard one, namely, the second order system is expanded to a larger system of first-order ODEs, then solved appropriately using the associated RK tableau. For most cases in this analysis (unless otherwise stated)

Please cite this article in press as: J.M. Lindquist et al., Klein–Gordon equation with advection on unbounded domains using spectral elements and high-order non-reflecting boundary conditions, Appl. Math. Comput. (2010), doi:10.1016/j.amc.2010.07.079

time integration is performed using a 4th order RK scheme using a time-step chosen to ensure a Courant number of 0.25, where the Courant number is defined:

$$\text{Courant number} = \frac{C_0 \triangle t}{\sqrt{(\triangle x)^2 + (\triangle y)^2}}.$$

Here, $\triangle x$ and $\triangle y$ are chosen as the minimum distance between any two points in the x- or y- directions respectively. Additionally, This choice is made since the interpolation points are not uniformly distributed when using spectral elements.

6. Numerical experiments

Several numerical experiments were performed to solve the KGE under advection with and without dispersion. In order to simplify the numerical simulation of the problem at hand, the KGE (3) is converted to a non-dimensional form as described in [32]. Using typical mesoscales in the ocean, the length scales were chosen O(100 km), vertical depth scales O(100 m) and the dispersion parameter f for Coriolis O(10^{-4} s^{-1}). In terms of advective velocities, Majda [32, p. 61] describes typical advective velocities as roughly $\frac{3}{100}$ that of the medium wave speed C_0. Here, we choose to challenge the boundary further by choosing faster advective velocities at $\frac{1}{10}$ that of the medium wave speed.

For experiments that follow, the reference wave speed is $C_0 = 1$, which allows the initial wave to propagate through the region of interest in a *reasonable* time for all experiments. Given the scale choices above yields a dispersion parameter f^2 of 0.1. Further, U and V are set to 0.0 or 0.1 under a two-dimensional Gaussian initial condition to test the formulation in a semi-infinite and infinite channel setting. The truncated domain Ω is defined on $x = [-2,2]$, $y = [-2,2]$ and the initial condition is given by:

$$\eta(x,y,0) = e^{-10\left(x^2-y^2\right)}, \quad \partial_t \eta(x,y,0) = 0.$$

In order to see the effect of the NRBC, we have compared our solution to the same one on a larger domain ($x = [-2,10]$ for the semi-infinite channel, and $x = [-6,6]$ for the infinite channel). This expanded domain reference solution replaces the NRBC with no-flux boundary conditions as well. The problem is then solved for $t = 3$ ensuring that the disturbance has propagated through the artificial boundary, yet has not had time to reach the no-flux boundary and pollute the reference solution.

To quantify the errors observed between the reference and NRBC solutions, we use the normalized L^2_Ω error defined as follows:

$$\|\text{error}\|_{L^2_\Omega} = \sqrt{\frac{\sum_{k=1}^{N_p} \left(\eta_k^N - \eta_k^R\right)^2}{\sum_{k=1}^{N_p} \left(\eta_k^R\right)^2}},$$

where η^N and η^R are the NRBC and reference solutions.

6.1. Semi-infinite channel

For the first experiment, the KGE is examined on a semi-infinite channel with the NRBC at $x_E = 2$ and constant advection with $U = 0.1$ and $V = 0$. In Fig. 5 we plot the reference solution on the top panel and the solution of the truncated domain

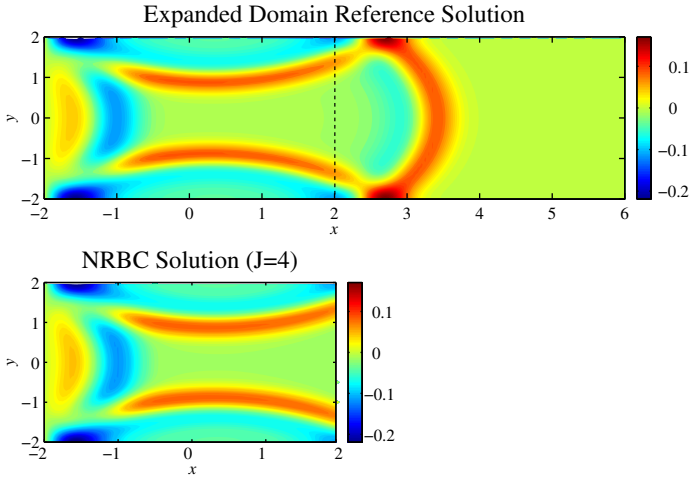

Fig. 5. Semi-infinite channel comparing extended domain reference solution and the NRBC solution. 4th order spectral elements using NRBC order $J = 4$ with advection velocities $U = 0.1$, $V = 0.0$ shown.

Please cite this article in press as: J.M. Lindquist et al., Klein–Gordon equation with advection on unbounded domains using spectral elements and high-order non-reflecting boundary conditions, Appl. Math. Comput. (2010), doi:10.1016/j.amc.2010.07.079

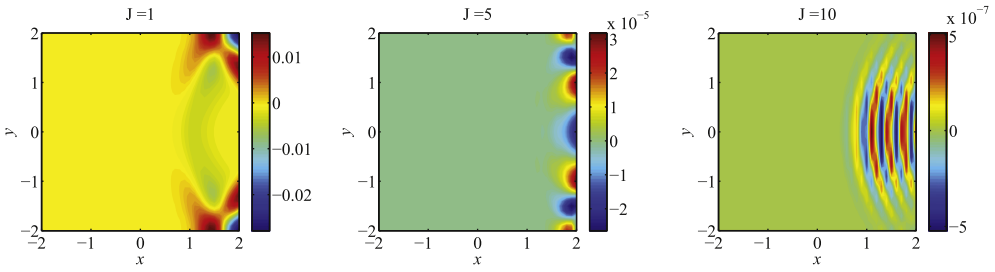

Fig. 6. Differences between the NRBC solutions ($J = 1, 5, 10$) and the truncated reference solution with $U = 0.1$, $V = 0.0$.

using the G–N NRBCs on the bottom panel. The solution on the truncated domain uses 4th order spectral elements on a 24×24 element grid, discretizing the domain into 9,409 points. The reference solution is computed on the extended domain using the same spectral order and 72×24 elements. Qualitatively speaking, the results show very little reflection using the combination of high-order elements and NRBC. The differences between the reference and NRBC solutions are shown in Fig. 6 for NRBC orders of 1, 5 and 10.

Quantitative results can be observed in Fig. 7 showing the error on Ω as a function of spectral and NRBC order ($J = 1, \ldots, 10, 15, 20$). The number of elements is adjusted for each spectral order to maintain an equal number of points (9,409) that the domain is discretized into. It is clear that increasing the NRBC order yields significant gains in accuracy, but by $J = 5$, the spatial discretization error dominates NRBC error in the low-order element (order 1 and 2) cases. However, by increasing the spectral order of the elements, this spatial discretization error decreases and allows the true accuracy of the NRBC to be realized. The Higdon boundary condition, while general in nature, implicitly assumes that by the time the wave pulse gets to the artificial boundary, it is traveling primarily as a *plane* wave normal to the boundary. The previous example, where the advective velocity was in the same direction as the channel, does not significantly challenge this assumption. In other words, to really test the value of the boundary condition, one must try advective velocities with some tangential component to the boundary. Fig. 8(c) and (d) show the same L^2_Ω plots for advection velocities in other directions, one being the contrived case where the advection is perfectly tangential to the NRBC. These L^2_Ω plots correspond with the contour plots directly below that show the comparative solutions. Examining these results, it is clear that the boundary condition-even when put to a test with a wave pulse containing a significant tangential component to the boundary-performs well. It is noted that the order of the error suffers slightly under diagonal advection when compared to its individual axial counterparts. This may be due to the additional terms activated in the interior and boundary formulations (19) and (20) when U and V are simultaneously non-zero.

6.2. Infinite channel

For the next set of experiments, the domain is an infinite channel with the NRBCs located at $x = \pm 2$. The set-up is similar to that of the semi-infinite channel. To begin, consider the Higdon boundary condition for the western boundary given by:

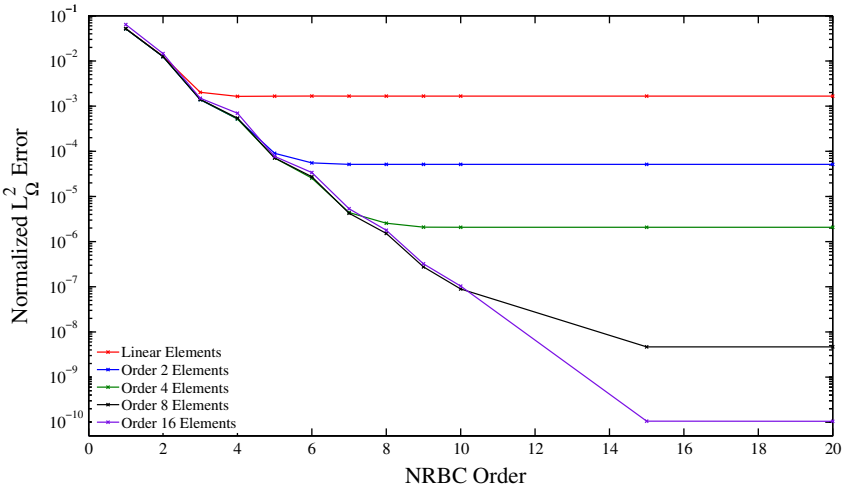

Fig. 7. Semi-infinite channel L^2_Ω error versus NRBC and spectral element order. Domain is discretized into 9,409 points for all spectral element orders with advection velocities $U = 0.1$, $V = 0.0$.

Please cite this article in press as: J.M. Lindquist et al., Klein–Gordon equation with advection on unbounded domains using spectral elements and high-order non-reflecting boundary conditions, Appl. Math. Comput. (2010), doi:10.1016/j.amc.2010.07.079

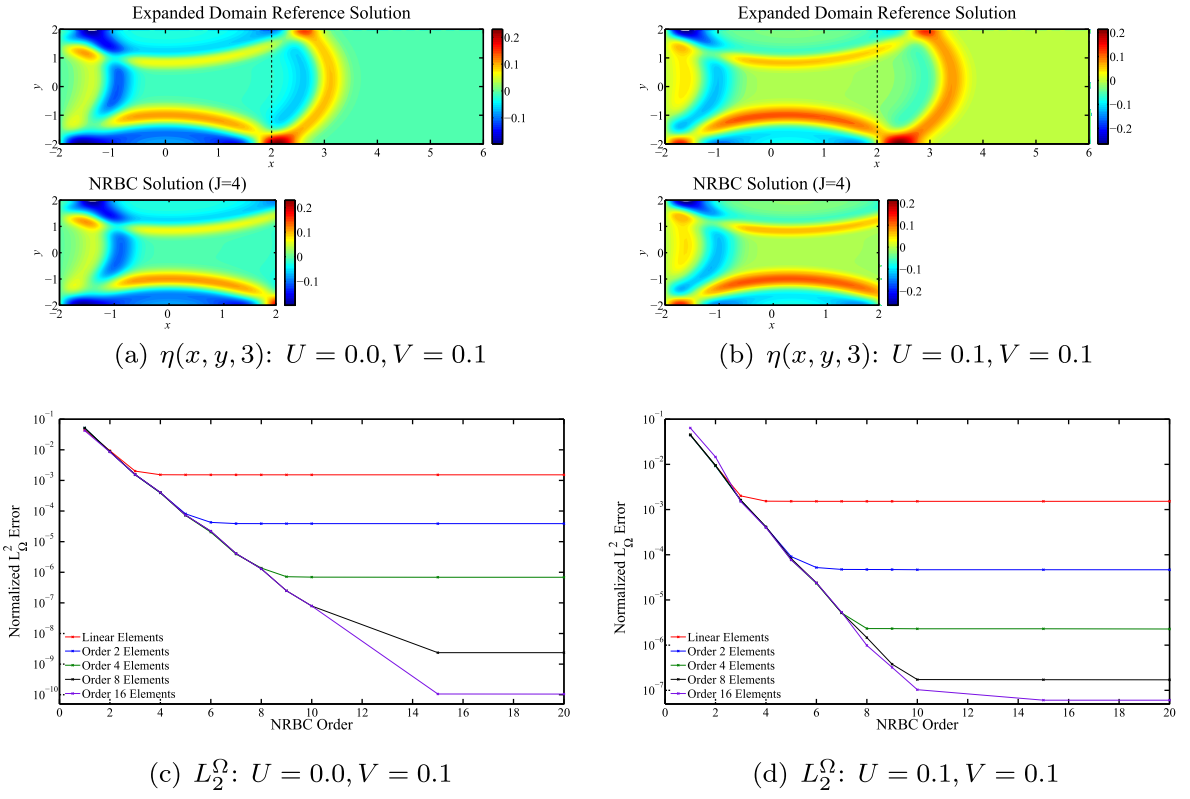

(a) $\eta(x, y, 3)$: $U = 0.0, V = 0.1$ (b) $\eta(x, y, 3)$: $U = 0.1, V = 0.1$

(c) L^{Ω}_2: $U = 0.0, V = 0.1$ (d) L^{Ω}_2: $U = 0.1, V = 0.1$

Fig. 8. Top Plots: Semi-infinite channel, 4th order spectral element ($J = 4$) contour plots showing $\eta(x,y,3)$ on extended and truncated domains. Domain is discretized into 9,409 points for all spectral element orders with advective velocities specified. Bottom Plots: Corresponding L^2_Ω error versus NRBC and spectral element order.

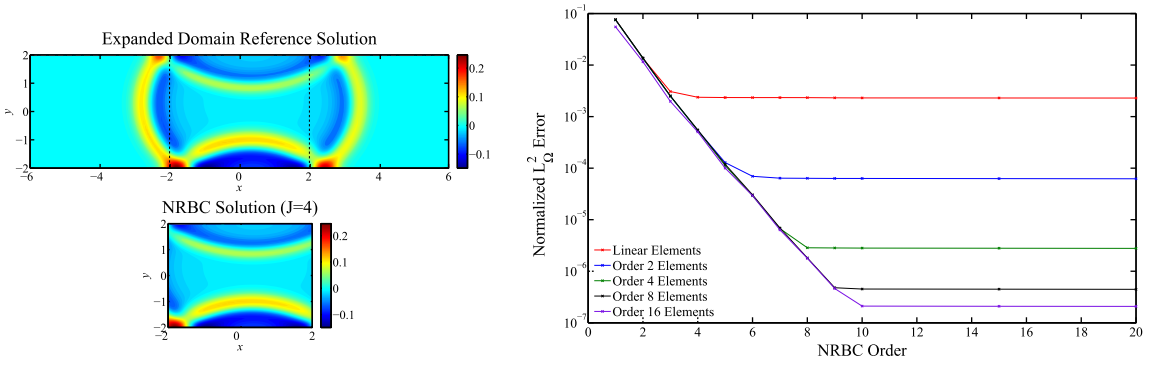

(a) $\eta(x, y, 3)$: $U = 0.1, V = 0.1$ (b) L^2_Ω: $U = 0.1, V = 0.1$

Fig. 9. Infinite channel comparing extended domain reference solution and the NRBC solution. 4th order spectral elements using NRBC order $J = 4$ with advection velocities $U = 0.1$, $V = 0.1$ shown.

$$H_J : \left[\prod_{j=1}^{J}\left(\partial_x - \frac{1}{C_j}\partial_t\right)\right]\eta = 0 \quad \text{on } \Gamma_E. \tag{31}$$

Using a similar strategy for introducing a set of auxiliary variables for the western NRBC, applying them to the KGE equivalent, then converting any normal derivatives on the boundary to time and tangential boundaries, results in another, very similar formulation that is directly incorporated into the weak form (18). The selection of parameters C_j follows the "convenient" choice as developed for the eastern boundary, namely to remove the second order in time auxiliary variable term. This choice is $C_j = C_0 - U$.

Please cite this article in press as: J.M. Lindquist et al., Klein–Gordon equation with advection on unbounded domains using spectral elements and high-order non-reflecting boundary conditions, Appl. Math. Comput. (2010), doi:10.1016/j.amc.2010.07.079

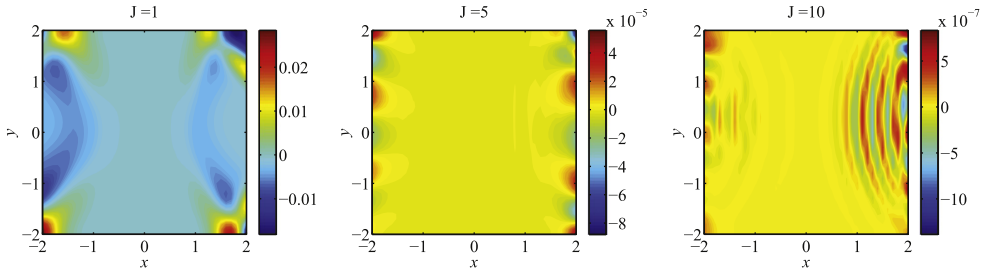

Fig. 10. Differences between the NRBC solutions ($J = 1, 5, 10$) and the truncated reference solution with $U = V = 0.1$.

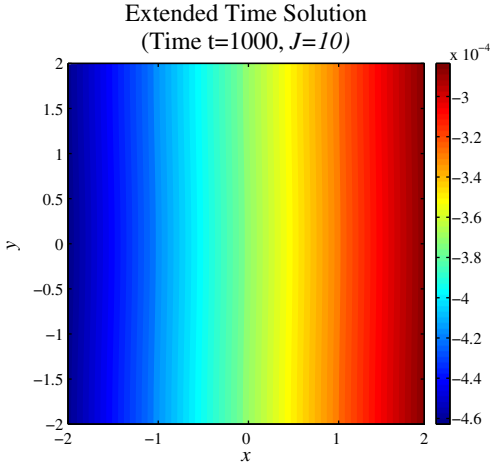

Fig. 11. Infinite channel, extended time solution ($t = 1000$). 4th order spectral elements using NRBC order $J = 4$ with advection velocities $U = 0.1$, $V = 0.0$ shown.

Similar experiments to those run in the semi-infinite channel were conducted using various advective velocities. In Fig. 9 we show the case where advection is towards the north-east corner of the domain. Again, qualitatively and quantitatively, the NRBC solution performs quite well. The differences between the reference and NRBC solutions are shown in Fig. 10 for NRBC orders of 1, 5 and 10.

6.3. Long term results

In many applications, there is concern for the stability and behavior of the NRBC scheme in the long term. In the final infinite channel experiment, we have run the KGE with $J = 10$ using 4th order basis functions (9,409 global points) for $t = 1000$. By this time the wave front has exited the truncated domain and the reference solution is expected to be zero throughout the entire domain. The differences between the reference ($\eta(x, y, 1000) = 0$) and the NRBC solution are shown in Fig. 11 are of order 10^{-4}. This figure shows that, as expected, absent sources in the domain, the wave front exits the domain with minimal reflection and in the long run, tends toward a steady state of zero. This would imply long term stability of the method when used in this context.

6.4. Effects of time integration technique

At the outset of this work, it was believed that at some point the improvements realized by improving the spatial discretization and NRBC would eventually be limited by the time integration scheme [33]. To this end, the order of the time integration scheme (RK2–RK10) was varied to examine the effects of time integration on the accuracy of the solution. As has already been presented, gains made by increasing the order of the NRBC halt for lower order spectral elements after $J = 5$. Even for high-order (order 8 and 16) spectral elements, the gains made by increasing the order of the NRBC are limited at some point using RK4. In [28] the authors showed that high-order time integration allowed boundary gains to improve solution quality for the KGE under zero advection. Here, in a problem incorporating advection, one might surmise that the changes in time would exaggerate any temporal discretization error.

For this experiment, consider the KGE on a semi-infinite domain with $\eta = 0$ on Γ_W. To ensure that any boundary or time effects are not masked by the interior discretization, we consider 8th order spectral elements discretized into 9,409 global

Please cite this article in press as: J.M. Lindquist et al., Klein–Gordon equation with advection on unbounded domains using spectral elements and high-order non-reflecting boundary conditions, Appl. Math. Comput. (2010), doi:10.1016/j.amc.2010.07.079

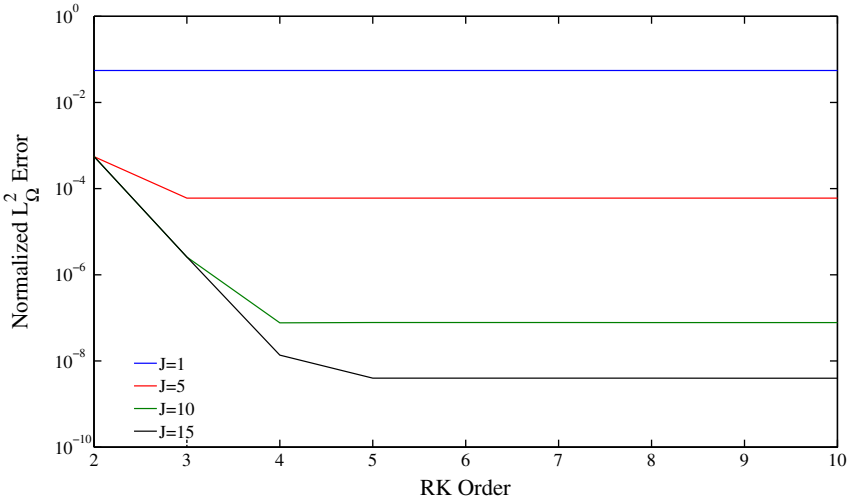

Fig. 12. Semi-infinite channel L^2_Ω error versus RK time integration order using various order NRBCs. Domain is discretized into 9,409 points for 8th order spectral elements with advection velocities $U = 0.75$, $V = 0.0$ and dispersion parameter $f^2 = 1$.

points. The Gaussian initial condition is used and is evaluated until $t = 3$. The reference solution in this case was computed as described previously, except that time integration was performed with a 10th order Runge–Kutta scheme (RK10) using a time-step chosen to ensure a Courant number of 0.1. Further, to exaggerate the issue of advection and dispersion, we consider the case where $U = 0.75$ and $f^2 = 1$.

As can be observed in Fig. 12, gains made by improving the time integration matter only if combined with high-order treatment of the boundary. Conversely-gains using high-order treatment of the boundary can only be realized if there is a *sufficiently* high-order treatment of the time integration. While this analysis conducted time integration using up to RK10 (18 stages), RK4 or RK5 appears to be sufficient in exploiting gains when using high-order boundary treatment. It should be noted that these results (error on the order of 10^{-9}) cannot be observed unless high-order treatment of the interior also accompanies the high-order treatment of the boundary and time. Several experiments were conducted which varied the order of the interior, boundary and time integration. The clear result was that without high-order treatment of all components in concert, convergence to the reference solution is stalled.

While these results are for a specific problem (KGE with advection), we believe that the principle of a balanced approach to all components (interior, boundary and time) is a sound, extensible procedure for any problem. If high-order treatment of any of the three components is missing, the high-order treatment of the other components is essentially wasted.

7. Conclusions

In this paper, we considered a reduced form of the shallow water equations on an infinite (channel) domain. Using the Givoli–Neta auxiliary variable formulation of the Higdon non-reflecting boundary conditions, we truncated the original infinite domain and developed the boundary conditions specific to the problem at hand. Using a high-order approach to the spatial discretization (spectral element), time integration (high-order Runge–Kutta) in concert with the high-order boundary treatment, we showed *exponential* convergence to the reference solution in various examples. These results suggest a balanced approach to dealing with truncation errors – namely, to make improvements in *all* components of the problem to see improved accuracy.

Future work includes extending these results to the quarter and open plane and extending all of this work to the full first-order SWE system. Challenges in extending this formulation primarily lie in developing appropriate corner compatibility conditions for the intersection of two boundaries. As the auxiliary variable formulation is itself a system of PDEs, well-posedness requires appropriate boundary conditions – which are not obvious – for each of the auxiliary variables when employed in a "corner-type" configuration. The authors have developed stable, low-order boundary conditions for the auxiliary variables for the KGE with advection, albiet with less impressive results, as well as alternative ways of handling the auxiliary variable formulation for an arbitrarily shaped convex boundary in [34]. Work is ongoing to further develop the auxiliary variable formulation that will maintain stable, high-order results in the quarter and open domain experiments.

Acknowledgements

The first author is indebted to the US Army for its support. The authors would like to express their appreciation to the Naval Postgraduate School for its support of this research. Finally, the authors wish to thank the reviewers for their helpful insights, suggestions and comments.

Please cite this article in press as: J.M. Lindquist et al., Klein–Gordon equation with advection on unbounded domains using spectral elements and high-order non-reflecting boundary conditions, Appl. Math. Comput. (2010), doi:10.1016/j.amc.2010.07.079

References

[1] D. Givoli, Non-reflecting boundary conditions, Journal of Computational Physics 94 (1) (1991) 1–29, doi:10.1016/0021-999(91)90135-8.
[2] B. Engquist, A. Majda, Radiation boundary conditions for acoustic and elastic calculations, Communications on Pure and Applied Mathematics 32 (3) (1979) 313–357, doi:10.1002/cpa.3160320303.
[3] A. Bayliss, E. Turkel, Radiation boundary conditions for wave-like equations, Communications on Pure and Applied Mathematics 33 (6) (1980) 707–725, doi:10.1002/cpa.3160330603.
[4] F. Collino, High order absorbing boundary conditions for wave propagation models. Straight line boundary corner cases, in: R. Kleinman et al. (Eds.), Proceedings of the Second International Conference on Mathematical & Numerical Aspects of Wave Propagation, SIAM, Delaware, 1993, pp. 161–171.
[5] S.V. Tsynkov, Numerical solution of problems on unbounded domains. A review, Applied Numerical Mathematics 27 (4) (1998) 465–532, doi:10.1016/S0168-9274(98)00025-7. Special issue on absorbing boundary conditions.
[6] D. Givoli, High-order local non-reflecting boundary conditions: a review, Wave Motion 39 (4) (2004) 319–326, doi:10.1016/j.wavemoti.2003.12.004.
[7] D. Givoli, Exact representations on artificial interfaces and applications in mechanics, Applied Mechanics Reviews 52 (11) (1999) 333–349, doi:10.1115/1.3098920.
[8] T. Hagstrom, Radiation boundary conditions for the numerical simulation of waves, Acta Numerica 8 (1999) 47–106, doi:10.1017/S0962492900002890.
[9] R.L. Higdon, Absorbing boundary conditions for difference approximations to the multi-dimensional wave equation, Mathematics of Computation 47 (176) (1986) 437–459.
[10] R.L. Higdon, Numerical absorbing boundary conditions for the wave equation, Mathematics of Computation 49 (179) (1987) 65–90.
[11] R.L. Higdon, Radiation boundary conditions for elastic wave propagation, SIAM Journal on Numerical Analysis 27 (4) (1990) 831–869.
[12] R.L. Higdon, Absorbing boundary conditions for elastic waves, Geophysics 56 (2) (1991) 231–241, doi:10.1190/1.1443035.
[13] R.L. Higdon, Absorbing boundary conditions for acoustic and elastic waves in stratified media, Journal of Computational Physics 101 (2) (1992) 386–418, doi:10.1016/0021-9991(92)90016-R.
[14] R.L. Higdon, Radiation boundary conditions for dispersive waves, SIAM Journal on Numerical Analysis 31 (1) (1994) 64–100, doi:10.1137/0731004.
[15] D. Givoli, B. Neta, High-order non-reflecting boundary conditions for dispersive waves, Wave Motion 37 (3) (2003) 257–271, doi:10.1016/S0165-2125(02)00074-4.
[16] B. Neta, V. van Joolen, J.R. Dea, D. Givoli, Application of high-order higdon non-reflecting boundary conditions to linear shallow water models, Communications in Numerical Methods in Engineering 24 (11) (2008) 1459–1466, doi:10.1002/cnm.1044.
[17] D. Givoli, B. Neta, High-order non-reflecting boundary scheme for time-dependent waves, Journal of Computational Physics 186 (1) (2003) 24–46, doi:10.1016/S0021-9991(3)00005-6.
[18] J.R. Dea, F.X. Giraldo, B. Neta, High-order non-reflecting boundary conditions for the linearized 2-d Euler equations: no mean flow case, Wave Motion 46 (3) (2009) 210–220, doi:10.1016/j.wavemoti.2008.11.002.
[19] D. Givoli, N. Beny, I. Patlashenko, Finite element analysis of time-dependent semi-infinite wave-guides with high-order boundary treatment, International Journal for Numerical Methods in Engineering 58 (13) (2003) 1955–1983, doi:10.1002/nme.842.
[20] T. Hagstrom, T. Warburton, A new auxiliary variable formulation of high-order local radiation boundary conditions: corner compatibility conditions and extensions to first-order systems, Wave Motion 39 (4) (2004) 327–338, doi:10.1016/j.wavemoti.2003.12.007.
[21] E. Bécache, D. Givoli, T. Hagstrom, High-order absorbing boundary conditions for anisotropic and convective wave equations, Journal of Computational Physics 229 (4) (2010) 1099–1129, doi:10.1016/j.jcp.2009.10.012.
[22] D. Givoli, T. Hagstrom, I. Patlashenko, Finite element formulation with high-order absorbing boundary conditions for time-dependent waves, Computer Methods in Applied Mechanics and Engineering 195 (29–32) (2006) 3666–3690, doi:10.1016/j.cma.2005.01.021.
[23] T. Hagstrom, A. Mar-Or, D. Givoli, High-order local absorbing conditions for the wave equation: extensions and improvements, Journal of Computational Physics 227 (6) (2008) 3322–3357, doi:10.1016/j.jcp.2007.11.040.
[24] A.T. Patera, A spectral element method for fluid dynamics: laminar flow in a channel expansion, Journal of Computational Physics 54 (3) (1984) 468–488, doi:10.1016/0021-9991(84)90128-1.
[25] F.X. Giraldo, M. Restelli, A study of spectral element and discontinuous galerkin methods for the Navier–Stokes equations in nonhydrostatic mesoscale atmospheric modeling: equation sets and test cases, Journal of Computational Physics 227 (8) (2008) 3849–3877, doi:10.1016/j.jcp.2007.12.009.
[26] V.J. van Joolen, B. Neta, D. Givoli, High-order boundary conditions for linearized shallow water equations with stratification, dispersion and advection, International Journal for Numerical Methods in Fluids 46 (4) (2004) 361–381, doi:10.1002/fld.754.
[27] L. Kucherov, D. Givoli, High-order absorbing boundary conditions incorporated in a spectral element formulation, Communications in Numerical Methods in Engineering, doi:10.1002/cnm.1188.
[28] J.M. Lindquist, B. Neta, F.X. Giraldo, A spectral element solution of the Klein–Gordon equation with high-order treatment of time and non-reflecting boundary, Wave Motion 47 (5) (2010) 289–298, doi:10.1016/j.wavemoti.2009.11.007.
[29] J. Pedlosky, Geophysical Fluid Dynamics, second ed., Verlag, New York, 1986.
[30] V.J. van Joolen, Application of higdon non-reflecting boundary conditions to shallow water models, Ph.D. Thesis, Naval Postgraduate School, Monterey, CA, 2003.
[31] V.J. van Joolen, B. Neta, D. Givoli, High-order higdon-like boundary conditions for exterior transient wave problems, International Journal for Numerical Methods in Engineering 63 (7) (2005) 1041–1068, doi:10.1002/nme.1322.
[32] A. Majda, Introduction to PDEs and Waves for the Atmosphere and Ocean, Courant Institute of Mathematical Sciences, New York, 2003.
[33] A. R. Curtis, High-order explicit Runge–Kutta formulae, their uses, and limitations, IMA Journal of Applied Mathematics 16, doi:10.1093/imamat/16.1.35.
[34] J.M. Lindquist, Unstructured high-order Galerkin-temporal-boundary methods for the Klein–Gordon equation with non-reflecting boundary conditions, Ph.D. Thesis, Naval Postgraduate School, Monterey, CA, 2010.

Please cite this article in press as: J.M. Lindquist et al., Klein–Gordon equation with advection on unbounded domains using spectral elements and high-order non-reflecting boundary conditions, Appl. Math. Comput. (2010), doi:10.1016/j.amc.2010.07.079